

Systematics of signature inversion in odd-odd nuclei in the mass regions  $A = 80$  and  $A = 160$ Renrong Zheng,<sup>1</sup> Shunquan Zhu,<sup>1</sup> Nanpu Cheng,<sup>2</sup> and Jiayan Wen<sup>3</sup><sup>1</sup>Department of Physics, Shanghai Normal University, Shanghai 200234, China<sup>2</sup>Department of Physics, Southwest Normal University, Chongqing 400715, China<sup>3</sup>Guangzhou Naval Vessel College, Guangzhou, China

(Received 4 October 1999; revised manuscript received 17 January 2001; published 18 June 2001)

Based on an axially symmetric rotor plus quasiparticles model, the study of the signature inversion (SI) in odd-odd nuclei in the mass region  $A = 160$  is extended to include the region  $A = 80$ . In spite of many differences between the two mass regions, the calculation results show that the possible SI mechanism, which has been confirmed by the calculation of odd-odd nuclei in the  $A = 160$  region (i.e., the competition between the  $n$ - $p$  interaction and the Coriolis force in low- $K$  space) is also appropriate for odd-odd nuclei in the  $A = 80$  region. This seems to indicate that there may be a universal mechanism of SI in odd-odd nuclei for different mass regions.

DOI: 10.1103/PhysRevC.64.014313

PACS number(s): 21.60.Ev, 27.70.+q

## I. INTRODUCTION

Signature inversion (SI) in odd-odd nuclei has attracted a lot of attention regarding both experimental and theoretical aspects. It has been observed in recent experiments that SI in odd-odd nuclei is a common phenomenon in the yrast band in three mass regions at  $A = 160$ , 130, and 80 [1–12]. On the other hand, to explain the experimental results, several mechanisms of SI have been suggested by various theoretical groups (e.g., [2,13–15]). These mechanisms differ to a certain degree [16], and most groups have performed corresponding calculations only for one of the three mass regions mentioned above. SI in odd-odd nuclei has been studied even less for the  $A = 80$  region. Therefore, there are still no answers to the question of what may cause the SI in odd-odd nuclei in the  $A = 80$  region and whether there is a universal description of the SI mechanism in odd-odd nuclei in different mass regions; and if there is a universal description, what is its nature?

We have developed a method for the two quasiparticles plus rotor model (QPRM) in studying odd-odd nuclei [16–22], in which special attention is paid to the model basis space so that it accounts for a  $\gamma$  vibration perturbation near axial symmetry. The nice agreements [16–21], between the model calculation results and the experimental values for real odd-odd nuclei in the  $A = 160$  region, have shown that the method is powerful to describe SI in odd-odd nuclei. And the SI mechanism drawn from the method [16–18] (i.e., the competition between the Coriolis force and the  $n$ - $p$  interaction in the low- $K$  model space) is reasonable too. In this paper we investigate the degree to which SI mechanism is universal by studying SI in odd-odd nuclei within mass regions  $A = 80$  and  $A = 160$ .

In Sec. II, the theoretical model will be briefly reviewed. The results and discussions will be presented in Sec. III, followed by the conclusions in the last section.

## II. OUTLINE OF THE THEORETICAL MODEL

Since the theory of the model has been described in Refs. [16–18], only the new aspects of the formulas related to

coefficients  $C_2$  and  $C_3$  (see below) are given in detail. The meanings of all the symbols in the present paper are the same as, e.g., in Ref. [16].

The model Hamiltonian  $H$  of an odd-odd nucleus takes the form

$$H = H_R + H_{sp} + H_{sn}, \quad (1)$$

where  $H_R$  stands for Hamiltonian of the rotor;  $H_{sp}$  and  $H_{sn}$  Hamiltonians belong to quasiproton and quasineutron located in two single  $j$  orbits outside the rotor, respectively, and

$$\begin{aligned} H_R &= \left( \frac{1}{2g} \right) \sum_{k=1}^2 (I_k - j_{nk} - j_{pk})^2 \\ &= \left( \frac{1}{2g} \right) [(I^2 - I_3^2) + (j_n^2 - j_{n3}^2) + (j_p^2 - j_{p3}^2)] \\ &\quad + C_2 \left( \frac{1}{2g} \right) (j_n - j_{p+} + j_{n+} j_{p-}) - C_3 \left( \frac{1}{2g} \right) \\ &\quad \times (I_+ j_{n-} + I_- j_{n+} + I_+ j_{p-} + I_- j_{p+}). \end{aligned} \quad (2)$$

It should be noted that in Eq. (2) there is a  $C_2$  factor on the left side of the second term concerning the  $n$ - $p$  coupling or the  $n$ - $p$  interaction term and a  $C_3$  factor in front of the third term that relates to the Coriolis force. Only when both  $C_2$  and  $C_3$  are equal to 1, is  $H_R$  an exact axial symmetry rotor.  $C_3$  is less than 1 that denotes the usual Coriolis attenuation factor in a calculation for a real nucleus. The  $C_2$  coefficient comes from consideration of the residual interaction: If  $C_2 > 1$ , then the surplus part (i.e.,  $C_2 - 1$ ) of the second term in  $H_R$  can be considered as a residual  $n$ - $p$  interaction, as the original second term in Eq. (2) has a form of  $n$ - $p$  interaction. That our calculations below will show the simplest way for counting  $n$ - $p$  residual interaction does work well, especially in the  $A = 80$  mass region, where the  $n$ - $p$  interaction is strong due to the same single- $j$  orbit occupied by both valence neutron and valence proton in a nucleus.

TABLE I. Values of parameters for yrast band calculations of nine odd-odd nuclei under consideration.

Nucleus	<sup>74</sup> Br	<sup>76</sup> Br	<sup>78</sup> Br	<sup>76</sup> Rb	<sup>78</sup> Rb	<sup>80</sup> Rb	<sup>82</sup> Y	<sup>84</sup> Y	<sup>86</sup> Nb
$g(\kappa^{-1})$	11.50	12.20	13.20	12.20	13.20	13.75	15.00	15.40	16.20
$\lambda_n(\kappa)$	-0.85	-0.75	-0.60	-0.85	-0.75	-0.60	-0.60	-0.45	-0.45
$\lambda_p(\kappa)$	-0.97	-0.97	-0.97	-0.90	-0.90	-0.90	-0.85	-0.85	-0.83
$C_2$	1.2	1.3	1.3	1.4	1.2	1.4	1.3	1.4	1.4
$C_3$	0.83	0.80	0.80	0.85	0.80	0.90	0.9	0.80	0.85
$\kappa=?$ keV	1200	1100	1200	1150	1240	1350	1300	1300	1200

The model space of an odd-odd nucleus in which we diagonalize Hamiltonian (1) is

$$\begin{aligned}
|IK\nu\rangle &= |IMK\nu_p\nu_n\rangle \\
&= \left(\frac{2I+1}{16\pi^2}\right)^{1/2} [D_{MK}^{I*}|\nu_p\rangle|\nu_n\rangle \\
&\quad + (-1)^{I-j_n-j_p} D_{M-K}^{I*} |-\nu_p\rangle|-\nu_n\rangle] \\
&= \left(\frac{2I+1}{16\pi^2}\right)^{1/2} \sum_{\Omega_p, \Omega_n} S_{\Omega_p, \nu_p}^{j_p} S_{\Omega_n, \nu_n}^{j_n} [D_{MK}^{I*} \chi_{\Omega_p}^{j_p} \chi_{\pm\Omega_n}^{j_n} \\
&\quad + (-1)^{I-j_p-j_n} D_{M-K}^{I*} \chi_{-\Omega_p}^{j_p} \chi_{\mp\Omega_n}^{j_n}], \quad (3)
\end{aligned}$$

where the product state  $|\nu_p\rangle|\nu_n\rangle$  is the eigenstate corresponding to the sum of two single particle eigenenergies

$$\varepsilon_\nu = \varepsilon_{\nu_p} + \varepsilon_{\nu_n}. \quad (4)$$

The matrix elements of  $H_R$  in the representation, in which the summation Hamiltonians of two quasiparticles  $H_{sn} + H_{sp}$  in Eq. (1) is diagonal, should be the matrix elements of  $H_R$  between two states of Eq. (3) times BCS factors relating to  $u$  and  $v$ , i.e.,

$$H_{\mu, \nu}^{KK'} = h_{\mu, \nu}^{KK'} (u_\mu^p u_\nu^p + v_\mu^p v_\nu^p) (u_\mu^n u_\nu^n + v_\mu^n v_\nu^n). \quad (5)$$

Solving the eigenvalue equation of  $H$  in this representation,

$$\sum_{K', \nu} (H_{\mu, \nu}^R + e_\nu \delta_{KK'} \delta_{\mu, \nu}) t_{K', \nu}^{(I, j_p, j_n)} = E^{(I, j_p, j_n)} t_{K, \mu}^{(I, j_p, j_n)}, \quad (6)$$

one will get the energy spectrum of  $H$  for a given spin  $I$ . The lowest energies for a series of definite  $I$  form a yrast band energy spectrum.

The model is indeed a  $\gamma=0$  case in triaxial quasiparticles plus rotor model.

### III. RESULTS AND DISCUSSIONS

#### A. The comparison of calculations with experiments for odd-odd nuclei in the mass region $A=80$

In present paper, nine yrast band spectra for nine odd-odd nuclei, namely, <sup>74-78</sup>Br, <sup>76-80</sup>Rb, <sup>82,84</sup>Y, and <sup>86</sup>Nb, are calculated with both odd-neutron and odd-proton located in the same single  $j=g_{9/2}$  orbit. According to time reversal invariance, the third components of  $j_n$  and  $j_p$  are  $\Omega_p = \Omega_n = 1/2$ ,

$-3/2, 5/2, \dots$ . The energy gap parameters are  $\Delta_p = \Delta_n = 0.6\kappa$  where  $\kappa$  is the energy unit [16] and  $K = -5, \dots, +5$  for the space bases formula (3). Other parameters are listed in Table I, where  $g$  is the moment of inertia;  $\lambda_p$  and  $\lambda_n$  are the Fermi energies of the valence proton and valence neutron, respectively;  $C_3$  indicates the Coriolis attenuation factor;  $C_2$ , strength coefficient of the  $n$ - $p$  interaction. It is worthwhile to mention that, except for the  $C_2$  and  $C_3$  coefficients, all parameters in the present paper are restricted by the corresponding physical meanings. They are not really free. For example: a  $\lambda$  means Fermi energy that is limited by the single particle occupation of the Nilsson level; the  $\kappa$  is limited by the deformation of the nucleus; and so on.

In Fig. 1 the calculation results of the spectra  $E(I) - E(I-1)$  vs spin  $I$  in the nine nuclei and the comparison of the computation results with the experiment data are shown. The nuclei in column (b) are the same as the corresponding subfigures of those in column (a) on the left. The parameters in the calculations are taken from Table I for column (a), with the only exception of  $C_2=1$  for all the calculations in column (b), i.e., the residual  $n$ - $p$  interaction is neglected in the theoretical results (dashed lines) of column (b).

As we can see from the subfigures of column (a), the theoretical results are consistent with experimental values. In the higher spin region, the calculation results coincide even quantitatively with the experimental data; the SI points, at which the signature of the zigzag lines starts to invert from normal at the higher spins to abnormal at the lower spins, are reproduced at the ‘‘right’’ spin positions in all nine nuclei; with discrepancies between theories and the experiments at few lower spins mainly with  $I < 9 = j_n + j_p$  in some lighter nuclei, i.e., the theoretical  $[E(I) - E(I-1)]$  values a little higher than that of experiments.

The comparisons of theoretical results in column (b) with that of the corresponding nuclei in column (a) tell us that the  $n$ - $p$  residual interaction has the effect mainly at lower spin regions. If  $C_2$  is equal to 1, which means without  $n$ - $p$  residual interaction as shown in the subfigures of column (b), the theoretical oscillation (dashed lines) keeps normal also at the lower spins as it does at higher spin region, which can be seen particularly clearly at the upper part of column (b) in nuclei <sup>86</sup>Nb, <sup>84</sup>Y, <sup>82</sup>Y, and <sup>80</sup>Rb. Without  $C_2 > 1$ , as in column (b), no experimental SI can be reproduced in all nine nuclei.

Opposite to column (b), the good agreements between calculations and experiments in column (a) indicate (1) the residual  $n$ - $p$  interaction in odd-odd nuclei plays an important

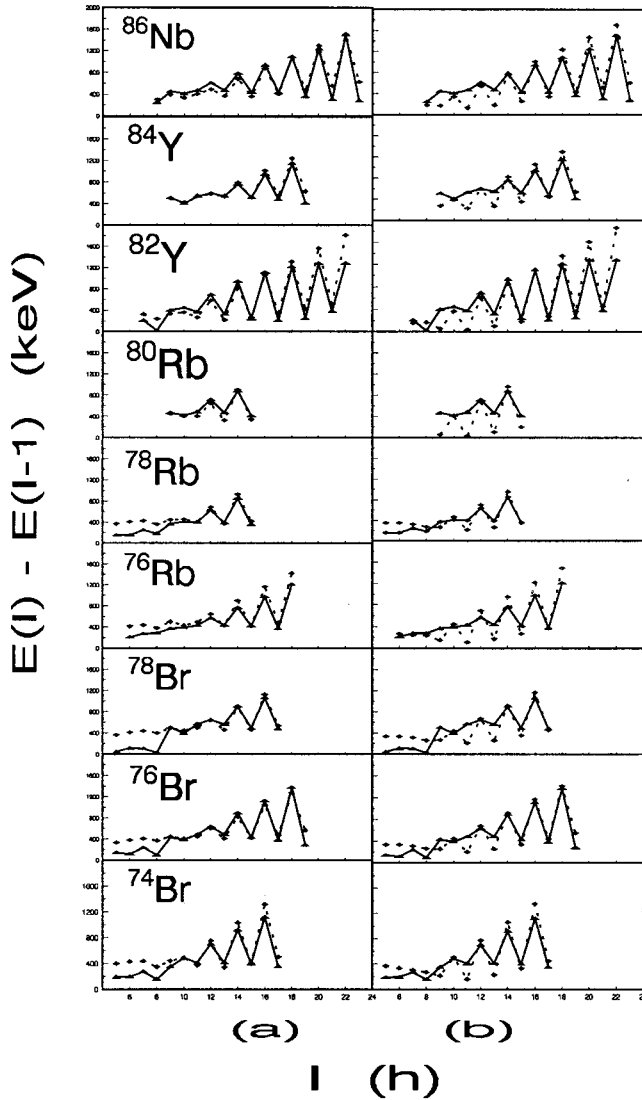


FIG. 1. The spectra of  $E(I) - E(I-1)$  vs spin  $I$  of nine odd-odd nuclei in the  $A=80$  region, and the comparison of calculation results with the experimental data. The only difference between columns (a) and (b) is the values of parameter  $C_2$ . The  $C_2$  values are taken from Table I, for column (a); and all  $C_2=1$  for the cases of column (b). Dashed lines indicate theoretical results and solid lines denote experimental values. (The concrete experiment data sources are from Refs. [3–11].)

role in the SI phenomenon at the lower spin area, (2) using  $C_2 > 1$  for taking the residual  $n-p$  interaction into account is the simplest but effective way in the present study.

### B. SI mechanism for odd-odd nuclei in the mass region of $A=80$

We have obtained the SI mechanism in odd-odd nuclei as “the competition between  $n-p$  interaction and Coriolis force in low- $K$  space” by analyzing the phase factors concerning the two competitive sides in our previous works [18,16]. In order to illustrate the SI mechanism further, we check the sensitivity of parameters with the calculation results and find that the most sensitive parameters in Table I are the Coriolis

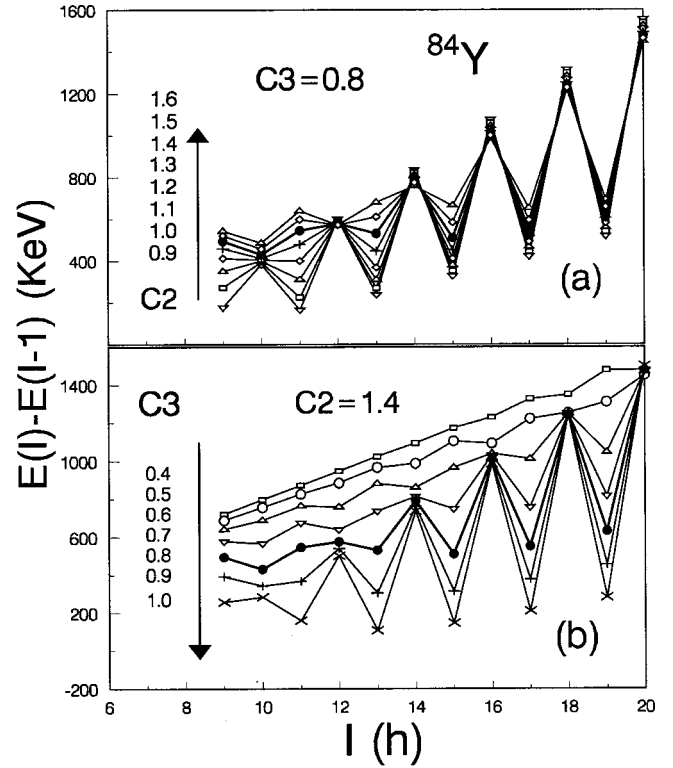


FIG. 2. A demonstration of the mechanism of SI in odd-odd nuclei in the  $A=80$  region taking the nucleus  $^{84}\text{Y}$  as an example. With fixed  $C_3=0.8$  and different  $C_2$  in (a) and fixed  $C_2=1.4$ , different  $C_3$  in (b).

attenuation coefficient  $C_3$  and the  $n-p$  interaction strength coefficient  $C_2$  as shown in Fig. 2. As the influence of parameters on the theoretical calculations is similar in all nine nuclei, we take  $^{84}\text{Y}$  nucleus from Fig. 1 as a concrete example. In Fig. 2, the same diagram of  $E(I) - E(I-1)$  vs  $I$  as in Fig. 1. is plotted with fixed magnitude of  $C_3$  and different values of  $C_2$  for the subfigure (a); and fixed  $C_2$ , different  $C_3$  for the subfigure (b).

One can obtain four characteristics from (a) of Fig. 2, where  $C_3=0.8$  is fixed at a “right” value.

(1) For a definite curve of certain  $C_2$  value in (a), the amplitude of the curve zigzag gets more and more small as the spin decreases. When  $C_2$  is not large enough, the phase of the curve zigzag keeps normal in the whole spin region, as in the typical situations of  $C_2=0.9, 1.0$ , and  $1.1$ .

(2) Different  $C_2$  parameters separate the ordinate values  $[E(I) - E(I-1)]$  of the same odd spin in (a) (relevant to the favorable states) from each other, and the separation is much larger when their corresponding abscissa values  $I$  are lower. This means the  $n-p$  interaction strength has an effect on the ordinate value mainly at the lower spins. For a definite odd spin, the amplitude of signature oscillation gets smaller as  $C_2$  coefficient increases.

(3) At certain  $C_2$  value (the thicker line with  $C_2=1.4$ ) and certain odd spin ( $I=11$ ), the phase of zigzag suddenly begins to invert from normal at the higher spin region to abnormal at the lower spin region, and one then obtains the reproduction of the experimental SI phenomenon [the same as  $^{84}\text{Y}$  in column (a) of Fig. 1].

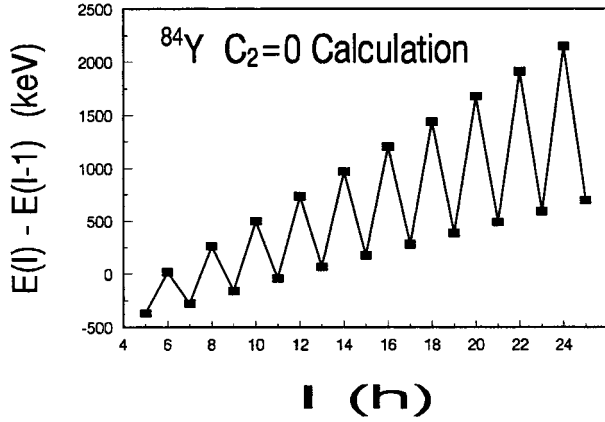


FIG. 3. The same as (b) of Fig. 2, but with  $C_3=0.8$  and  $C_2=0$ , both fixed. This figure shows that pure Coriolis force (without  $n-p$  interaction) causes the signature splitting normal in the whole spin region, and the lower the spin  $I$ , the smaller the amplitude of signature oscillation.

(4) After the ‘‘right’’  $C_2=1.4$ , if the value of parameter  $C_2$  increases continuously, the spin value of SI starting point becomes bigger, just like, for example, the curve with  $C_2=1.6$  the starting SI point  $I=13$ , which is bigger than the experimental data of  $I=11$ .

Since  $C_2$  is the  $n-p$  interaction strength coefficient and  $C_3$  the Coriolis strength, the (a) of Fig. 2 denotes that  $n-p$  interaction has the function of reducing the amplitude of zigzag curve made by Coriolis force (see Fig. 3), the reduction is especially strong at the lower spin area, as the amplitude of the curve staggering is weaker originally. This induces the phase of the curve vibration inversion, i.e., SI.

Figure 2(b), tells us another story: When the  $n-p$  interaction is fixed, the amplitude of the curve vibration tends to be smaller in the whole spin area as the Coriolis force becomes weaker (i.e.,  $C_3$  decreases). When  $C_3$  gets the right value (the little thicker line of  $C_3=0.8$ ), the phase of the vibration keeps normal at the high spin area and starts inversion from  $I=11$  at the lower spin area. When the  $C_3$  coefficient is too small, the curve vibration disappears almost in the whole spin region like a few curves in the upper part of (b) with, e.g.,  $C_3=0.4, 0.5$ .

The (a) and (b) of Fig. 2 combine together to make a physical picture that SI phenomenon of a definite nucleus in the experiment is a balance of Coriolis force and  $n-p$  interaction at least in the present QPRM method.

### C. A similarity of SI mechanism in odd-odd nuclei in the mass region $A=160$ to that of $A=80$

In Fig. 4,  $S(I)=[E(I)-E(I-1)]-\{[E(I+1)-E(I)]+E(I-1)-E(I-2)]/2$  values are plotted vs spins  $I$  for three odd-odd nuclei in the  $A=160$  region. Here, instead of  $[E(I)-E(I-1)]$  as in Fig. 1, the  $S(I)$  is used for amplifying signature oscillation amplitudes that are too small in the diagram of  $E(I)-E(I-1)$  vs  $I$  at lower spins in the  $A=160$  region. The main parameters used in theoretical calculation are listed in the first three nuclei of Table II for column (a), with the only exception of all  $C_2=1$  for calcu-

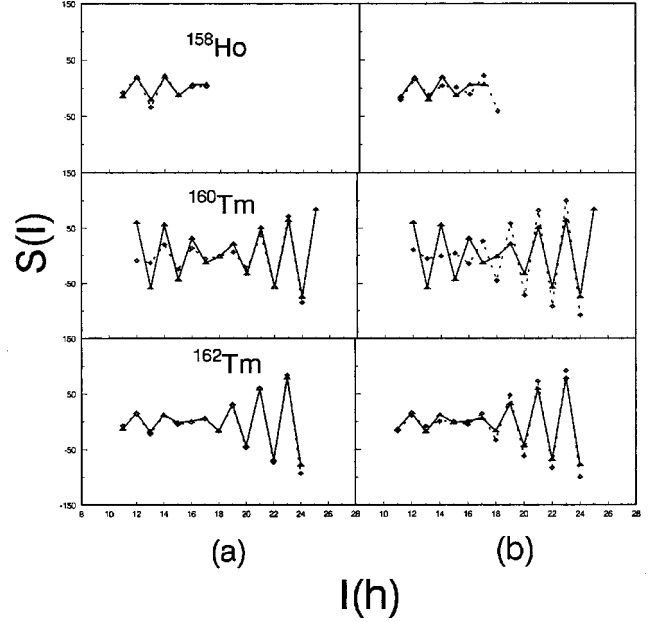


FIG. 4. The same as Fig. 1, but with perpendicular axis  $S(I)=[E(I)-E(I-1)]-\{[E(I+1)-E(I)]+E(I-1)-E(I-2)]/2$  and three nuclei for the  $A=160$  mass region. The parameters are taken from the first three nuclei of Table II for column (a); and with the only exception of all  $C_2=1$  for column (b).

lation (dashed line) in column (b), the other details related to the calculation in Fig. 4 are the same as described in [16].

Figure 4 shows the same consequence as Fig. 1: with proper  $n-p$  residual interaction as in column (a) of Fig. 4, the calculation can reproduce the experiment SI nicely. And a discrepancy between theory and experiment appears without  $n-p$  residual interaction as shown in column (b).

It should be mentioned that in general, the  $n-p$  interaction in odd-odd nuclei is weaker in the  $A=160$  mass region than that in the  $A=80$  region, as the valence neutron and valence proton of the former are located in two different single- $j$  orbits ( $i13/2$  for neutron,  $h11/2$  for proton), while they are located in the same  $j=g9/2$  orbit for nuclei in the  $A=80$  mass region. Thus the SI phenomenon of some nuclei in the  $A=160$  area, such as  $^{156}\text{Tb}$ ,  $^{160}\text{Ho}$ ,  $^{164}\text{Tm}$ , can also be reproduced by making the parameter  $C_2=1$  [16–18].

The parameters of theoretical calculation (dashed line) in (a) of Fig. 5 are listed in the fourth nuclei column in Table II. The same effects in (b) and (c) of Fig. 5 as in Fig. 2 are

TABLE II. The same as Table I, but for three odd-odd nuclei in the  $A=160$  region.

Nucleus	$^{158}\text{Ho}$	$^{160}\text{Tm}$	$^{162}\text{Tm}$	$^{156}\text{Tb}$
$g(\kappa^{-1})$	62.60	63.10	63.35	55.00
$\lambda_n(\kappa)$	-0.90	-0.90	-0.87	-0.9
$\lambda_p(\kappa)$	-0.42	-0.41	-0.41	-0.45
$C_2$	1.15	1.3	1.1	1.0
$C_3$	0.80	0.83	0.80	0.80
$\kappa=?$ keV	2000	2000	2000	1800

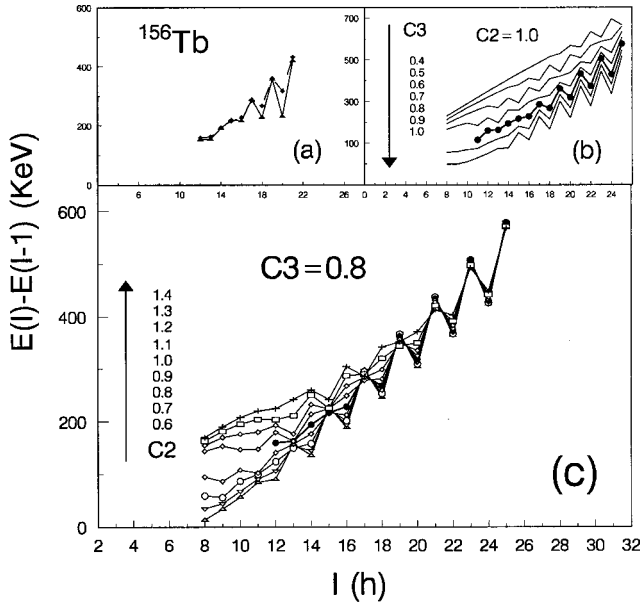


FIG. 5. The subfigure (a) is the same as in Fig. 1 but with the parameters taken from fourth nucleus ( $^{156}\text{Tb}$ ) of Table II. The subfigures (b) and (c) are the same as (b) and (a) of Fig. 2, respectively, but for nucleus  $^{156}\text{Tb}$ .

shown. The subfigure (b) of Fig. 5 corresponds to the (b) of Fig. 2, and the subfigure (c) of Fig. 5 to the (a) of Fig. 2.

The basic similarity between (b), (a) of Fig. 2 and (b), (c) of Fig. 5 shows that “the  $n$ - $p$  interaction competes against the Coriolis force in low- $K$  space for inverting the phase of signature vibration as SI mechanism in double odd nucleus” is available for both  $A = 160$  and  $A = 80$  regions. And the strong  $n$ - $p$  interaction pushes SI point to a higher spin, the weaker  $n$ - $p$  interaction gives a lower inversion point.

#### D. Differences in SI phenomena in odd-odd nuclei between $A = 160$ and $A = 80$ mass regions illustrated by (b), (a) of Fig. 2 and (b), (c) of Fig. 5

One can see from the comparing of zigzag lines of the higher parameters of  $C_3 = 1.0, 0.9, 0.8$  in (b) of Fig. 5 with the lower part on the (b) of Fig. 2; and the comparison of  $C_2 = 1.1$  to  $1.4$  at the lower spins in (c) of Fig. 5 to the upper and left part on the (a) of Fig. 2, that the separation of  $E(I) - E(I-1)$  values corresponding unfavorable states in the  $A = 160$  mass region (at  $I = \text{odd}$ ) are larger than those of  $A = 80$  region (at  $I = \text{even}$ ).

The different ordinate scales of Figs. 2 and 5 show much more smaller signature vibration in the  $A = 160$  region than that of in the  $A = 80$  region.

In one word, there exist a stronger  $n$ - $p$  interaction and a stronger signature oscillation in the  $A = 80$  region than that of in the  $A = 160$  region.

Another difference of the SI in two different mass regions is shown by the comparison between the two subfigures in Figs. 2 and 5 themselves. The separations among lines caused by changing  $C_3$  (Coriolis force) in (b) of Fig. 2 are larger than that by varying  $C_2$  ( $n$ - $p$  interaction) in (a) of the same Fig. 2 in the whole spin region of the nucleus of  $^{84}\text{Y}$ ;

while the opposite is true for the nucleus  $^{156}\text{Tb}$  in Fig. 5, i.e., the separations induced by  $C_2$  particularly at the lower spins in the (c) of Fig. 5 can be compared with that by  $C_3$  as shown in (b) of Fig. 5. This means, in the  $A = 160$  region the  $n$ - $p$  interaction plays a more important role than the Coriolis force in the competition between the two sides, while in the  $A = 80$  region the contrary is held, because of the greater influence from the Coriolis force than that from  $n$ - $p$  interaction as shown in Fig. 2. Therefore,  $C_2$  variation from nucleus to nucleus can be described nicely only in the  $A = 160$  region (see Sec. III E below) by connecting the systematic features of the SI points with the  $n$ - $p$  interaction.

#### E. A possible explanation of the systematic features of SI points in the mass region of $A = 160$

The SI phenomena in double-odd nuclei in the  $A = 160$  region have the features “In a chain of isotopes, the inversion point shifts to a lower spin regularly with the increasing neutron number; while in a chain of isotones, the inversion point shifts to a higher spin regularly with the increasing proton number” [22,23].

The results of our method and the comparing with the experimental data for odd-odd nuclei in the  $A = 160$  region are shown in Fig. 6. The number on the lower right corner of each subfigure is the magnitude of  $C_2$  used in calculations for the nucleus. As we can see, in a chain of isotopes (all subfigures in the same row) the magnitude of  $C_2$  shifts to smaller value with the increasing neutron number regularly, smaller  $C_2$  stands for weaker  $n$ - $p$  interaction, thus it corresponds to a lower spin of the inversion point; while in a chain of isotones (all subfigures in the same column) the  $C_2$  value shifts to the bigger magnitude with the increasing proton number regularly, bigger  $C_2$  means stronger  $n$ - $p$  interaction, hence it gives a higher spin inversion point. The  $C_2$  value variation coincides with the systematic features of the SI points in the  $A = 160$  region directly.

How the  $C_2$  value is related to the shell filling in the  $A = 160$  region is shown in Fig. 7, schematically. The variation of  $C_2$  for a chain of isotopes is indicated in column (a),  $\lambda_p$  being the common proton Fermi surface in the orbit of  $j = h11/2$ , the dashed lines stand for Fermi energies of valence neutrons in different nuclei within the isotopes, the direction of the arrow at the left side of the figure shows that the larger the neutron number in the nucleus, the higher the neutron Fermi energy, i.e., the higher the filling of the valence neutron, and hence the larger the energy gap between the  $\lambda_p$  and  $\lambda_n$ , which gives the weaker  $n$ - $p$  interaction, correspondingly the smaller  $C_2$  value and a lower spin of the inversion point. This explains the systematic feature in a chain of isotopes mentioned above.

On the contrary to column (a), in a chain of isotones as shown in column (b) of Fig. 7, the energy gaps between the various  $\lambda_p$  and the common  $\lambda_n$  in the  $j = i13/2$  orbit become smaller when the proton number in the nucleus increases, which connects to the stronger  $n$ - $p$  interaction, i.e., the larger  $C_2$  value and a higher spin of the inversion point.

The calculations in Fig. 6 tell us that in the yrast bands of odd-odd nuclei in the  $A = 160$  region, the  $n$ - $p$  interaction

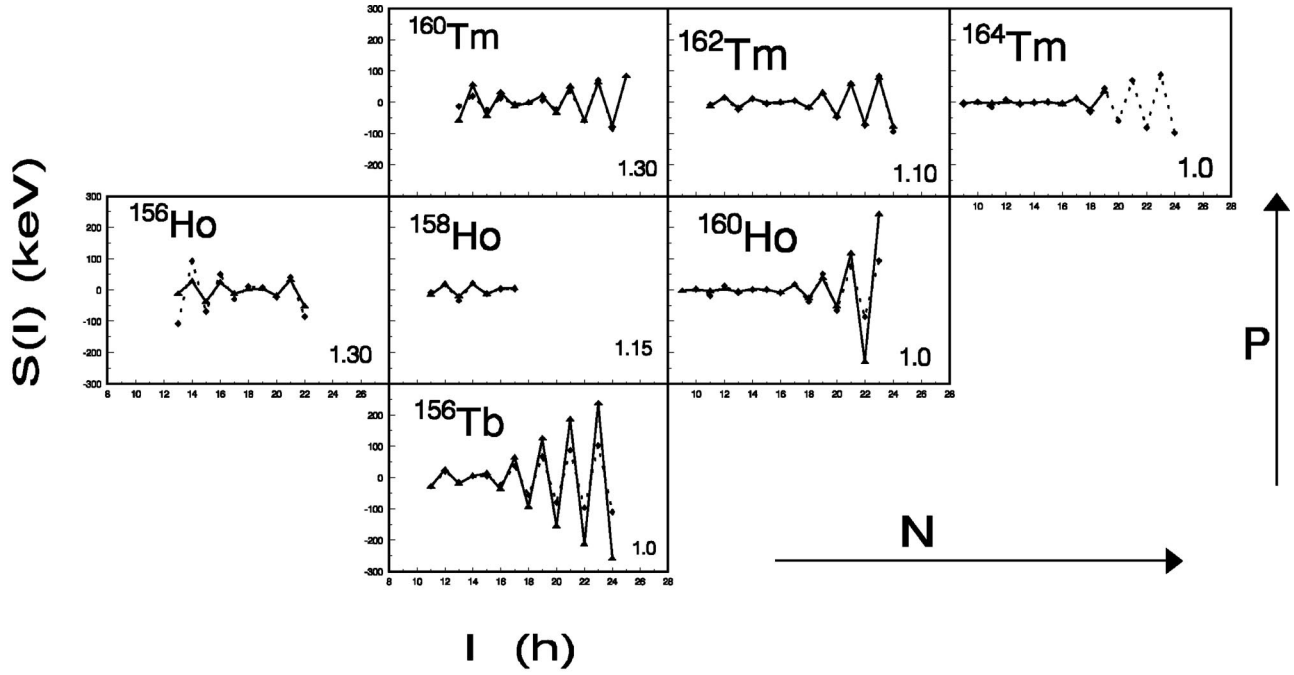


FIG. 6. The same as column (a) of Fig. 4, with the  $C_2$  value written on the right lower corner for each nucleus that shows the regulation of the  $C_2$  variation in chains of isotopes and isotones.

coefficient ( $C_2$ ) increases with the  $N-Z$  (neutron number minus proton number) number decreasing because the gap between  $n$ -Fermi energy and  $p$ -Fermi level becomes smaller with the decreased  $N-Z$  number.

Unfortunately in the  $A=80$  region, there is neither a remarkable systematic feature of the inversion points in the experiments nor a rule of the  $n-p$  interaction as in the  $A=160$  region. It might be necessary to have more reliable

experimental data for inducing the regulation of the experiments and analyzing the variation of  $n-p$  interaction more carefully.

IV. CONCLUSIONS

From the physics point of view, there exist several differences in odd-odd nuclei between  $A=80$  and  $A=160$  regions.

In the  $A=160$  region, (1) the valence proton and valence neutron are located in two different parities and different  $j$  orbits, (2) the difference number of  $N-Z$  is more than 20, (3) the valence  $n-p$  interaction is not very strong compared to odd-odd nuclei in the  $A=80$  region, but it plays a main role in the competition with the Coriolis force as shown in Fig. 5.

Therefore as long as the deformation of the nucleus is not very large, the strength of  $n-p$  interaction (i.e.,  $C_2$  coefficient) can be illustrated clearly by looking at the energy gaps between two valence neutron and valence proton as shown in Fig. 7.

Opposite to  $A=160$  region, the odd-odd nuclei in the  $A=80$  region show the following. (1) The valence proton and valence neutron are located in one single  $j$  orbit, (2) the difference number of  $N-Z$  is less than 10 (from 2 to 8, in Table I). Therefore strength of  $n-p$  interaction in odd-odd nucleus in the  $A=80$  region seems strongly effected by the quasiparticle character of the nucleons in the nucleus. (3) The rule that “the lower spin of inversion point in a chain of isotopes corresponds to weaker  $n-p$  interaction” illustrated by (a) of Fig. 2 is still kept in general (e.g., as in nuclei  $^{74}\text{Br}$ ,  $^{78}\text{Rb}$ , and  $^{82}\text{Y}$ , with SI point  $I=9$ , and all other nuclei in Table I have another SI point:  $I=11$ ).

Although many differences induced by the mass differ-

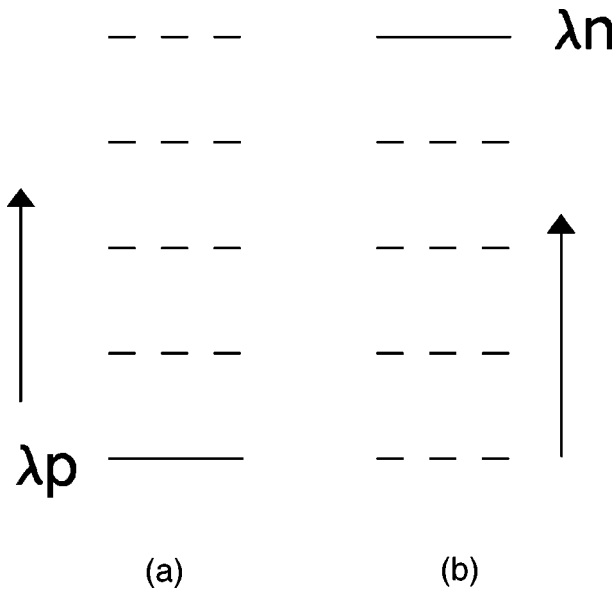


FIG. 7. A schematic diagram for variation of gaps between Fermi surfaces  $\lambda_n$  and  $\lambda_p$  in odd-odd nuclei in the  $A=160$  mass region. Column (a) for nuclei within a chain of isotopes, (b) for nuclei within a chain of isotones.

ence between the two mass regions, such as configurations, parities of yrast band, strengths of the  $n$ - $p$  interactions, etc., the mechanism of the SI in odd-odd nuclei in the  $A=80$  region as stated in Sec. III is the same as in the  $A=160$  region [16]. This hints the mechanism of SI presented in this paper might be a universal one for various mass regions of odd-odd nuclei.

In addition to the phase factor analysis described in Ref. [16], the graph method demonstrated by Figs. 2, 3, and 5 provides another way to interpret the cause of the SI in odd-odd nuclei that verifies the correctness of the SI mechanism further.

The systematic feature of the inversion point in odd-odd nuclei in  $A=160$  region is explained by the strength rule of  $n$ - $p$  interaction (i.e.,  $C_2$  value) related to shell filling.

#### ACKNOWLEDGMENTS

This work was supported by the National Natural Science Foundation of the People's Republic of China. The authors thank Professor Liao Jizhi from Sichuan University of China with whom we had helpful discussions.

- 
- [1] A. J. Kreiner *et al.*, Phys. Rev. Lett. **43**, 1150 (1979).
  - [2] R. Bengtsson *et al.*, Nucl. Phys. **A389**, 158 (1982).
  - [3] J. Doring *et al.*, Phys. Rev. C **47**, 2560 (1993).
  - [4] D. F. Winchell *et al.*, Phys. Rev. C **55**, 111 (1997).
  - [5] E. Landufo *et al.*, Phys. Rev. C **54**, 626 (1996).
  - [6] D. Rudolph *et al.*, Phys. Rev. Lett. **76**, 376 (1996).
  - [7] A. Harder *et al.*, Phys. Rev. C **51**, 2932 (1996).
  - [8] R. A. Kaye *et al.*, Phys. Rev. C **54**, 1038 (1996).
  - [9] S. K. Tabel *et al.*, Nucl. Phys. **A632**, 3 (1998).
  - [10] S. Chattopadhyay *et al.*, Phys. Rev. C **49**, 116 (1994).
  - [11] S. L. Labor *et al.*, Phys. Rev. C **56**, 142 (1997).
  - [12] J. Doering *et al.*, Phys. Rev. C **59**, 71 (1999).
  - [13] I. Hamamoto, Phys. Lett. B **235**, 221 (1990).
  - [14] K. Hara and Y. Sun, Nucl. Phys. **A531**, 221 (1991).
  - [15] N. Tajima, Nucl. Phys. **A572**, 365 (1994).
  - [16] Zheng Renrong *et al.*, Phys. Rev. C **56**, 175 (1997).
  - [17] Shunquan Zhu *et al.*, High Energy Phys. Nucl. Phys. **20**, 455 (1996).
  - [18] Shunquan Zhu and Renrong Zheng, Chin. Phys. Lett. **13**, 504 (1996).
  - [19] Renrong Zheng and Shunquan Zhu, Int. J. Mod. Phys. E **8**, 131 (1999).
  - [20] Pu Yunwei *et al.*, Chin. Phys. Lett. **15**, 480 (1998).
  - [21] Jiayan Wen, Renrong Zheng, and Shunquan Zhu, Acta Phys. Sin. **48**, 433 (1999).
  - [22] Jiayan Wen, Master thesis, Southwest China Normal University, 1999 (in Chinese).
  - [23] Yunzuo Liu *et al.*, Phys. Rev. C **52**, 2514 (1995).